

Copyright © 1991, by the author(s).  
All rights reserved.

Permission to make digital or hard copies of all or part of this work for personal or classroom use is granted without fee provided that copies are not made or distributed for profit or commercial advantage and that copies bear this notice and the full citation on the first page. To copy otherwise, to republish, to post on servers or to redistribute to lists, requires prior specific permission.

**ON THE UNIVERSE OF STABLE CELLULAR  
NEURAL NETWORKS**

by

Leon O. Chua and Chai Wah Wu

Memorandum No. UCB/ERL M91/31

24 April 1991

CONFIDENTIAL

**ON THE UNIVERSE OF STABLE CELLULAR  
NEURAL NETWORKS**

by

Leon O. Chua and Chai Wah Wu

Memorandum No. UCB/ERL M91/31

24 April 1991

**ELECTRONICS RESEARCH LABORATORY**

College of Engineering  
University of California, Berkeley  
94720

**ON THE UNIVERSE OF STABLE CELLULAR  
NEURAL NETWORKS**

by

Leon O. Chua and Chai Wah Wu

Memorandum No. UCB/ERL M91/31

24 April 1991

**ELECTRONICS RESEARCH LABORATORY**

College of Engineering  
University of California, Berkeley  
94720

# On the Universe of Stable Cellular Neural Networks\*

Leon O. Chua and Chai Wah Wu†

## Abstract

Cellular Neural Networks(CNN) is a novel analog circuit architecture with many desirable features. This paper extends previous stability results of CNN's to include classes of strictly sign-symmetric and acyclic templates. We show that most of the  $3 \times 3$  strictly sign-symmetric templates are stable almost everywhere, with the unknown templates reduced to three cases. We also introduce signed interaction graphs which is useful for obtaining results concerning stability and irreducibility of CNN templates.

## 1 Introduction

Cellular neural networks(CNN), a new type of analog circuits, was invented recently and shown to have many desirable properties [1]. CNN's consist of many parallel analog processors computing in real time. One desirable feature is that these processors, arranged in a two-dimensional grid, only have local connections, which lent themselves easily to VLSI implementations. The connections between these processors are determined by a cloning template, which describes the strength of nearest neighbor interconnections. The cloning templates we will consider are all space invariant, meaning that each processor has the same relative connections.

Some important applications of CNN's are in the area of binary image processing, where several templates has been discovered for edge detection, noise removal, image thinning, motion detection and other image processing functions([2],[10],[12]). For proper operation of such templates, a CNN must be completely stable, i.e. for all initial conditions, the states  $\rightarrow e$  as  $t \rightarrow \infty$ , where  $e$  is some, usually among many, dc equilibrium point. In the original paper [1], complete stability has been proved for CNN's with symmetric templates.

---

\*This work is supported in part by the Office of Naval Research under grant N00014-89-J-1402, by the National Science Foundation under Grant MIP 86-14000, and by the Semiconductor Research Corporation.

†Department of Electrical Engineering and Computer Sciences, University of California, Berkeley, CA 94720

CNN's form a special subclass of systems of differential equations, and by using results obtained for competitive-cooperative systems, a larger class of templates can be shown to be stable. In [3], a class of non-symmetric templates has been shown to be stable except for a set of measure zero, using results in [4].

This paper extends these results, and shows that most strictly sign-symmetric templates are stable almost everywhere. We will also show that acyclic templates are completely stable. We will also introduce the use of signed interaction graphs in analyzing templates and show several results relating to these graphs.

## 2 Preliminary definitions

A CNN is governed by the following set of differential equations [1]:

$$C \frac{dv_{x_{ij}}(t)}{dt} = -\frac{1}{R_x} v_{x_{ij}}(t) + \sum_{k,l} A(i,j;k,l) v_{y_{kl}}(t) + \sum_{k,l} B(i,j;k,l) v_{u_{kl}}(t) + I \quad (1)$$

where  $v_{x_{ij}}$ ,  $v_{u_{ij}}$  and  $v_{y_{ij}}$  denotes the state voltage, input voltage and output voltage of a cell, respectively. We assume that the input is constant and the A-template is space-invariant; i.e. for all  $i, j, k, l, m$  and  $n$ ,  $A(i, j; k, l) = A(i + m, j + n; k + m, l + n)$

$v_y = \hat{f}(v_x) = \frac{1}{2} [|v_x + 1| - |v_x - 1|]$ . We will often use a smooth ( $C^1$ ) approximation of that piecewise linear function in our stability analysis.

**Definition 2.1** A dynamical system  $\dot{x} = F(x)$ ,  $F \in C^1$  is cooperative if for all  $i \neq j$ :

$$\frac{\partial F_i(x)}{\partial x_j} \geq 0 \quad (2)$$

**Definition 2.2** A dynamical system is irreducible if for all  $i \neq j$ , there exists a chain of consecutive indices  $i = k_0, \dots, k_m = j$  such that:

$$\frac{\partial F_{k_r}(x)}{\partial x_{k_{r-1}}} \neq 0, \quad r = 1, 2, \dots, m. \quad (3)$$

**Definition 2.3** A dynamical system is stable almost everywhere if the set of initial values in which the system does not converge to a constant equilibrium point has Lebesgue measure zero.

Note that a dynamical system satisfying definition 2.3 is *not* necessarily completely stable since it may contain unstable limit cycles or other exotic trajectories. This weaker form of stability is easier to prove than complete stability, and is all that we need in practice.

Throughout this paper, “*stable*” is used in the sense of Hirsh[5], who called it “*convergent*”

**Definition 2.4** *A cloning template  $A(i, j; k, l)$  is positive if  $A(i, j; k, l) \geq 0$  for all  $(i, j) \neq (k, l)$ .*

**Definition 2.5** *A cloning template  $A(i, j; k, l)$  is cell-linking if the non-zero values of  $A(i, j; k, l)$  are located so that any two cells in the entire cell array can be connected by a sequence of cells with non-zero template values connecting them. (see [9])*

In order to better visualize the connections between cells, let us introduce a useful tool in analyzing CNN’s.

### 3 Signed interaction graphs

We associate to each A-template a labeled directed graph  $\Gamma$ . The nodes of  $\Gamma$  will be the individual cells, with a directed edge from cell( $k, l$ ) to cell( $i, j$ ) if and only if  $A(i, j; k, l) \neq 0$ . The label associated with that edge will be the sign of  $A(i, j; k, l)$ . We will also call that edge positive or negative, depending on the sign. As in [6], we will call  $\Gamma$  the signed interaction graph. This graph allows us to see how the cells are connected to each other, directly and indirectly. Table 1 list some templates along with their graphs ([2],[8],[9],[11]). Instead of attaching labels to edges, positive edges will be shown black, and negative edges will be shown gray.

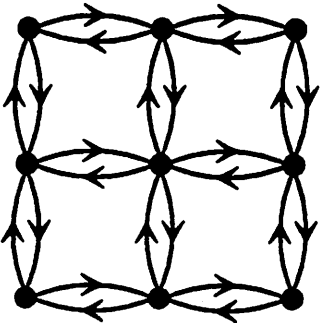
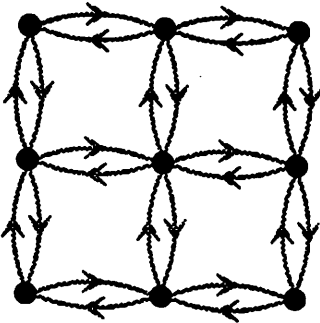
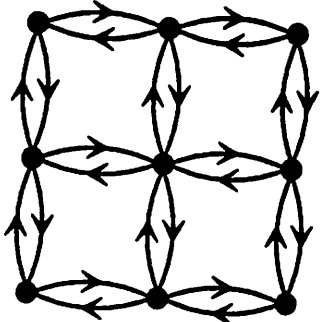
Name	A-template	graph									
(a) noise removal	<table><tr><td>0.0</td><td>1.0</td><td>0.0</td></tr><tr><td>1.0</td><td>4.0</td><td>1.0</td></tr><tr><td>0.0</td><td>1.0</td><td>0.0</td></tr></table>	0.0	1.0	0.0	1.0	4.0	1.0	0.0	1.0	0.0	
0.0	1.0	0.0									
1.0	4.0	1.0									
0.0	1.0	0.0									
(b) edge detection	<table><tr><td>0.0</td><td>-0.5</td><td>0.0</td></tr><tr><td>-0.5</td><td>2.0</td><td>-0.5</td></tr><tr><td>0.0</td><td>-0.5</td><td>0.0</td></tr></table>	0.0	-0.5	0.0	-0.5	2.0	-0.5	0.0	-0.5	0.0	
0.0	-0.5	0.0									
-0.5	2.0	-0.5									
0.0	-0.5	0.0									
(c) Hole filler	<table><tr><td>0.0</td><td>1.0</td><td>0.0</td></tr><tr><td>1.0</td><td>2.0</td><td>1.0</td></tr><tr><td>0.0</td><td>1.0</td><td>0.0</td></tr></table>	0.0	1.0	0.0	1.0	2.0	1.0	0.0	1.0	0.0	
0.0	1.0	0.0									
1.0	2.0	1.0									
0.0	1.0	0.0									

Table 1



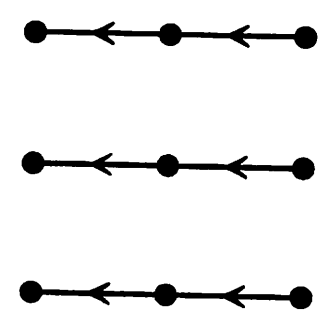
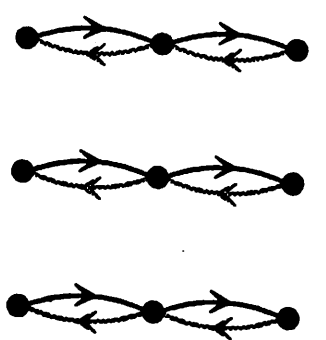
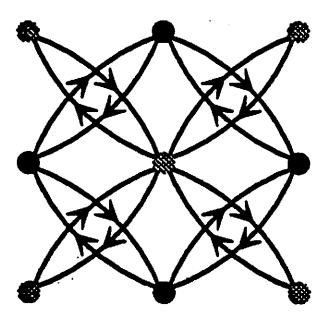
Name	A-template	graph									
horizontal shadow detector (d)	<table> <tr><td>0.0</td><td>0.0</td><td>0.0</td></tr> <tr><td>0.0</td><td>2.0</td><td>2.0</td></tr> <tr><td>0.0</td><td>0.0</td><td>0.0</td></tr> </table>	0.0	0.0	0.0	0.0	2.0	2.0	0.0	0.0	0.0	
0.0	0.0	0.0									
0.0	2.0	2.0									
0.0	0.0	0.0									
connected component detector (e)	<table> <tr><td>0.0</td><td>0.0</td><td>0.0</td></tr> <tr><td>1.0</td><td>2.0</td><td>-1.0</td></tr> <tr><td>0.0</td><td>0.0</td><td>0.0</td></tr> </table>	0.0	0.0	0.0	1.0	2.0	-1.0	0.0	0.0	0.0	
0.0	0.0	0.0									
1.0	2.0	-1.0									
0.0	0.0	0.0									
(f)	<table> <tr><td>1.0</td><td>0.0</td><td>1.0</td></tr> <tr><td>0.0</td><td>2.0</td><td>0.0</td></tr> <tr><td>1.0</td><td>0.0</td><td>1.0</td></tr> </table>	1.0	0.0	1.0	0.0	2.0	0.0	1.0	0.0	1.0	
1.0	0.0	1.0									
0.0	2.0	0.0									
1.0	0.0	1.0									

Table 1 (continued)

Name	A-template	graph									
(g)	<table border="1"> <tr> <td>0.0</td><td>0.0</td><td>0.0</td></tr> <tr> <td>0.0</td><td>2.0</td><td>2.0</td></tr> <tr> <td>0.0</td><td>2.0</td><td>0.0</td></tr> </table>	0.0	0.0	0.0	0.0	2.0	2.0	0.0	2.0	0.0	
0.0	0.0	0.0									
0.0	2.0	2.0									
0.0	2.0	0.0									

Table 1 (continued)

If we look at the shadow detector and its graph, we see that the rows are disconnected. This means that the state of a cell in a certain row cannot affect or depend on the state of a cell in another row. So we can consider each row as an independent 1-dimensional CNN and analyze its behavior separately. Furthermore, all the edges point to the left, meaning that cells influence the state of cells to their left and not vice versa. All this is consistent with the operation of a horizontal shadow detector.

**Definition 3.1** A directed graph is irreducible if for all  $i \neq j$ , there is a directed path from node  $i$  to node  $j$ .

A cell-linking template corresponds to  $\Gamma$  being irreducible. The hole-filler is a cell-linking template, i.e. the corresponding  $\Gamma$  is irreducible. This means that every cell can influence every other cell. This is consistent with the fact that hole-filling is a global property. Whether a cell is part of a hole or not depends on cells around it, possibly quite a distance away.

A disconnected directed graph cannot be irreducible. Hence, the directed graph (d), (e) and (f) in table 1 are reducible. Even a *connected* digraph may be reducible. An example of a connected digraph that is reducible is shown in (g) of table 1.

**Definition 3.2** A directed graph is symmetric if an edge from node  $i$  to node  $j$  implies an edge exists from node  $j$  to node  $i$ .

**Definition 3.3**  $E$ , a subgraph of  $\Gamma$ , is said to be maximally irreducible if any irreducible subgraph of  $\Gamma$  containing  $E$  is equal to  $E$ .

$\Gamma$  can be partitioned into maximally irreducible subgraphs. A symmetric  $\Gamma$  can always be partitioned into one or more maximally irreducible subgraphs that are disconnected from each other. To prove that assertion, let cell  $i$  be a cell in maximally irreducible subgraph 1 and cell  $j$  a cell in maximally irreducible subgraph 2. If there is an edge from cell  $i$  to cell  $j$ , then by the symmetry property there must be an edge from cell  $j$  to cell  $i$ . Every element in subgraph 1 has a path to cell  $i$ , hence to cell  $j$ , hence to every element in subgraph 2 and vice versa. So the union of subgraph 1 and subgraph 2 is irreducible. Since subgraph 1 and subgraph 2 are maximally irreducible, this implies that subgraph 1 = subgraph 1  $\cup$  subgraph 2 = subgraph 2. So the maximally irreducible subgraphs of  $\Gamma$  are not connected to each other.

Consider graph (a) in table 1. This graph is symmetric and consist of a maximally irreducible connected subgraph; namely, itself. Consider next graph (f) in table 1. The graph is symmetric and can be seperated into two totally disconnected subgraphs corresponding to the two maximally irreducible subgraphs. In table 1, nodes corresponding to the two maximally irreducible subgraphs are colored black and gray respectively. In a sense this CNN is equivalent to two independent CNN's operating on a state space that is interleaved.

**Definition 3.4** *A directed graph is called acyclic if it has no cycles, i.e. there are no set of nodes  $v_1, \dots, v_j, v_{j+1}$  all distinct, except for  $v_{j+1} = v_1$  such that there is an edge from  $v_i$  to  $v_{i+1}$ ,  $i = 1, \dots, j$ .*

If a graph is acyclic then a path from node  $i$  to node  $j$  implies no paths from node  $j$  to node  $i$ . Intuitively, this means that the dependence of cells are only in one direction. There is no indirect feedback through other cells. The graph of the shadow detector is an example of an acyclic graph.

The stability results obtained in [3] and in this paper are dependent only on the A-template or equivalently,  $\Gamma$ . This is useful as it allows us to determine the stability of some CNN by analyzing solely its signed interaction graph. For example,  $\Gamma$  can be used is to determine whether the template is cell-linking or not.

## 4 Test for irreducibility of $\Gamma$

A cell-linking CNN template indicates that the operation performed is global; the state of a cell depends on the states of all other cells. To test whether a CNN template is cell-linking, essentially one needs to check whether  $\Gamma$  is irreducible. One way to do that is to start with any node and check whether the maximally irreducible subgraph containing that node is equal to  $\Gamma$  itself.  $\Gamma$  is irreducible if and only if each node has at least one path to all its immediate neighbors. Because  $\Gamma$  is generated by a space-invariant template, we can give simpler sufficient conditions for a CNN being cell-linking.

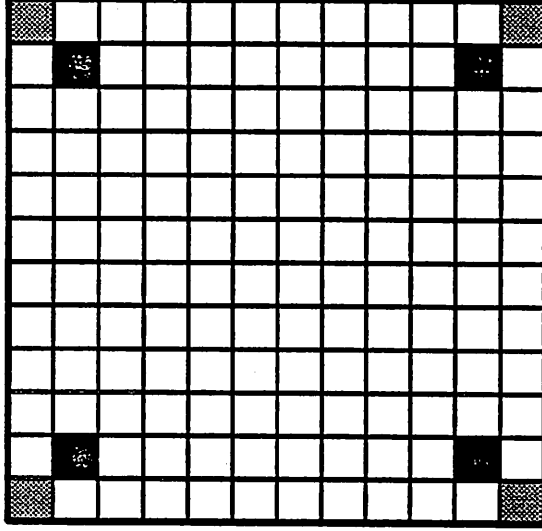


Figure 1: Paths from cells shown in black and gray, as specified in theorem 4.1 provide sufficient conditions for  $\Gamma$  being irreducible.

One such condition is given by our next theorem, where we only need to check the paths emanating from the 4 corners in the boundary of the CNN (shown in gray in Fig. 1) as well as those of 4 other “near-corner” cells adjacent to the corner cells along the diagonals (shown in black in Fig. 1).

**Theorem 4.1** *Given an A-template, if in the signed interaction graph  $\Gamma$  generated by an  $M \times N$  CNN utilizing that template, each of the 4 “near-corner” cells in  $\Gamma$  has paths going to all of its 8 immediate neighbors, and if each of the 4 “corner” cells in  $\Gamma$  has a path to its corresponding “near-corner” cell, then a CNN of at least  $(2M - 2) \times (2N - 2)$  cells utilizing the same A-template, will generate an irreducible sign interaction graph.*

**Proof:** Consider a CNN of  $(2M - 2) \times (2N - 2)$  cells and its signed interaction graph  $\Gamma$  divided into 4 quadrants as shown in Fig. 2. All we need to show is that every node in  $\Gamma$  has paths to all its immediate neighbors. Consider first the lower-left quadrant. We define an augmented quadrant as a quadrant

augmented with one more layer of cells. For example, the cells outside the lower-left quadrant with a dot in the center together with the lower-left quadrant form the corresponding augmented quadrant. By a boundary cell we mean a cell on the boundary of the  $(2M - 2) \times (2N - 2)$  array. A path from the “near-corner” cell to one of its immediate neighbor is shown as connecting node 1 through 8 in Fig. 2. Because of space invariance, any path in  $\Gamma$  can be shifted and still remain a valid path in  $\Gamma$  as long as the entire path stays within  $\Gamma$ . Because the augmented quadrant is  $M \times N$ , the path from the “near-corner” cell lies entirely within the augmented quadrant. Consider a path from the “near-corner” cell to its immediate neighbours shifted so that it starts from another cell in the quadrant. Because the quadrant is  $(M - 1) \times (N - 1)$ , the maximum amount of shift will be a distance of  $M - 3$  up and  $N - 3$  to the right and the path will remain within  $\Gamma$ . For example, the two paths in Fig. 2 starting from node 9 and 10 are just shifted version of the path from node 1 to 8. They lie completely within  $\Gamma$  and are therefore valid paths in  $\Gamma$ . It is clear from Fig. 2 that every cell in that quadrant that is not a boundary cell has a path to its immediate neighbors. They are essentially shifted versions of a “near-corner” cell. They also have paths to every cell in the quadrant. Using similar arguments for the other quadrants, it follows that every cell in the  $\Gamma$  that is not a boundary cell has paths to its immediate neighbors and thus to every cell in  $\Gamma$ .

Consider next a cell on the bottom boundary of the lower-left quadrant. The lower left corner cell has a path, call it  $p_1$ , towards the upper right neighbors, lying completely inside the augmented quadrant. The distance between the cell in question and the lower left corner cell is at most  $N - 2$ . Therefore the path  $p_1$  shifted so that it start at this cell will still lie entirely within  $\Gamma$ . The shifted path will end at the cell’s upper right neighbor which is not a boundary cell. Since a cell not on the boundary has paths to every cell in the graph, this cell on the bottom boundary also has path to every cell in the graph, in particular its immediate neighbors. In Fig. 3, node 3 has a path to node 4 since node 1 has a path to node 2. Node 4 is not a boundary cell, so node 4 has paths to every other cell in  $\Gamma$ . Therefore, node 3 has paths to every other cell in  $\Gamma$ . A similar argument holds for a cell on the left boundary in the quadrant. Therefore every cell in the quadrant has a path to its immediate neighbors. The boundary cells in the other quadrants follow a similar reasoning. It follows that  $\Gamma$  is irreducible. It is clear that the signed interaction graphs of even larger CNN’s (using the same A-template) will also be irreducible ■

When  $M = N = 3$ , we have the following corollary:

**Corollary 4.1** *Given a A-template, if in the  $\Gamma$  of a  $3 \times 3$  CNN utilizing that A-template, the center cell has paths to all the other cells, and if each corner cell has a path to the center cell, then the signed interaction graph generated by a  $4$  by  $4$  (or bigger) CNN utilizing that A-template, is irreducible.*

We conjecture that if the hypothesis of corollary 4.1 is satisfied then the

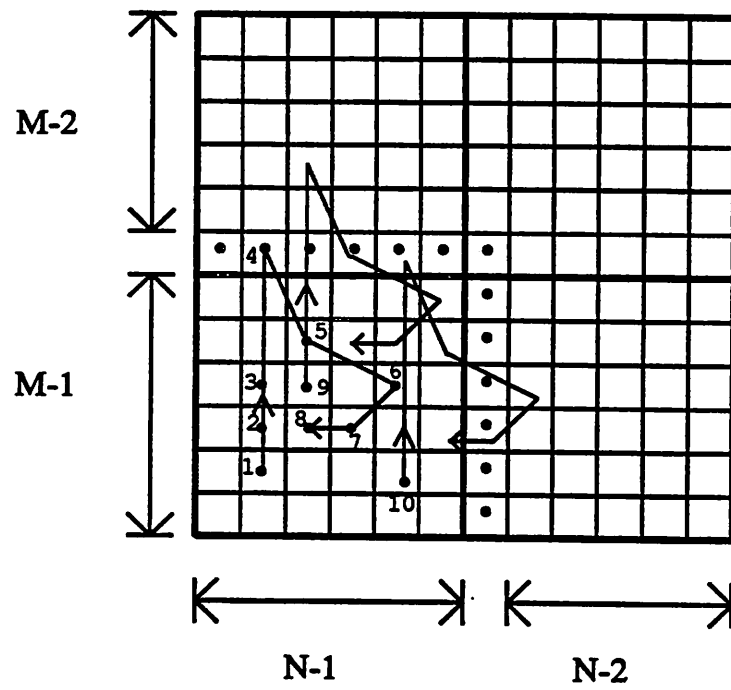


Figure 2: Each cell that is not a boundary cell has paths going to its neighbors.

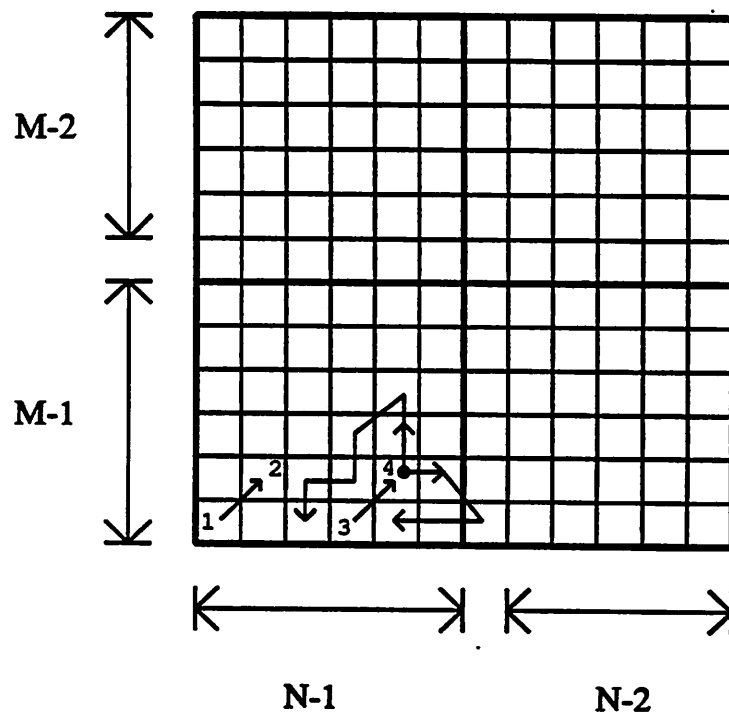


Figure 3: A cell on the boundary has paths to its immediate neighbors.

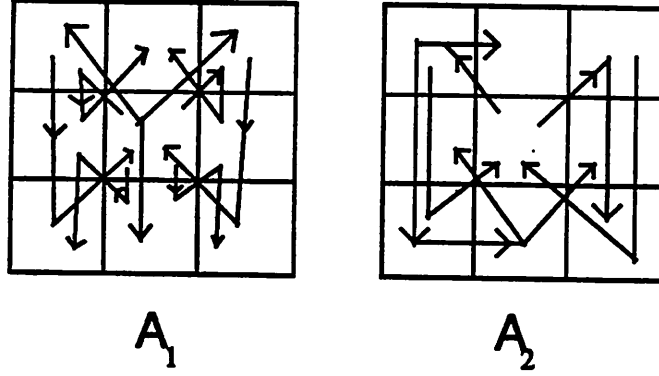


Figure 4: The requirement for irreducibility is satisfied for template  $A_1$  and  $A_2$ .

signed interaction graph generated by any size CNN is irreducible. As an example, let us analyze two A-templates described by:

0	1	0
0	A	0
1	0	1

$A_1$

0	0	1	0	0
0	0	0	0	0
0	1	A	0	0
0	1	0	1	0
0	0	0	0	0

$A_2$

As shown in Fig. 4, the signed interaction graphs of those templates for a  $3 \times 3$  CNN satisfy the requirements stated above. Therefore both templates are cell-linking in a CNN bigger than  $4 \times 4$ .<sup>1</sup>

## 5 State transformations

In [3], stability results has been obtained for CNN's with positive cell-linking templates. We will extend these results by finding state transformations that produce a transformed system similar in form to a CNN with positive cell-linking templates.

<sup>1</sup> actually the templates are cell-linking for any size CNN's.



Consider again the state equation of a  $M \times N$  CNN:

$$C \frac{dv_{x_{ij}}(t)}{dt} = -\frac{1}{R_x} v_{x_{ij}}(t) + \sum_{k,l} A(i,j;k,l) v_{y_{kl}}(t) + \sum_{k,l} B(i,j;k,l) v_{u_{kl}}(t) + I \quad (4)$$

As in [3], let us repack the state variables  $v_{x_{ij}}$  of the CNN into a vector  $\tilde{x}$  of size  $MN$ . Similarly, let us repack the input and output variables  $v_{u_{ij}}$  and  $v_{y_{ij}}$  into  $\tilde{u}$  and  $\tilde{y}$ , respectively (using the same ordering as that for  $\tilde{x}$ ). The invertible ordering will be called  $\sigma$ , i.e.  $\tilde{x}_{\sigma(i,j)} = v_{x_{ij}}$ . Without loss of generality, let  $R_x = 1, C = 1$  and the state equations assumes the form:

$$\dot{\tilde{x}} = F(\tilde{x}) = -\tilde{x} + \tilde{A}f(\tilde{x}) + \tilde{B}\tilde{u} + \tilde{I} \quad (5)$$

where  $\tilde{A}$  and  $\tilde{B}$  are  $MN \times MN$  matrices containing the coefficients  $A(i,j;k,l)$  and  $B(i,j;k,l)$  respectively.  $\tilde{I}$  is a constant vector of length  $MN$  and  $f_i(x) = \hat{f}(x_i) \approx \frac{1}{2} [|x_i + 1| - |x_i - 1|]$  for  $i = 1, \dots, MN$ .<sup>2</sup> By our choice of  $f(x)$ ,  $\frac{\partial f_i(x)}{\partial x_i} > 0$ , so for  $i \neq j$

$$\frac{\partial F_i(\tilde{x})}{\partial \tilde{x}_j} = \tilde{A}_{ij} \frac{\partial f_j(\tilde{x})}{\partial \tilde{x}_j} > 0 \Leftrightarrow \tilde{A}_{ij} > 0 \quad (6)$$

So the system is cooperative if and only if  $\tilde{A}$  has only nonnegative off-diagonal elements. CNN's whose templates are not positive have a corresponding  $\tilde{A}$  matrix that contains some *negative* off-diagonal elements. Our goal is to find a suitable transformation that produces an equivalent dynamical system that is cooperative and irreducible. We will consider a type of transformation where only the sign of some strategically chosen states are changed. Changing the signs of state variables amounts to multiplying the state vector by  $J = \text{diag}\{(-1)^{n_1}, (-1)^{n_2}, \dots, (-1)^{n_k}\}$ , where  $k = MN$ , the size of the state vector, and  $n_i \in \{0, 1\}$ . Setting  $J\tilde{x}' = \tilde{x}$ , the state equation transforms as follows:

$$\begin{aligned} \dot{\tilde{x}} = F(\tilde{x}) = -\tilde{x} + \tilde{A}f(\tilde{x}) + \tilde{B}\tilde{u} + \tilde{I} &\Leftrightarrow \\ J\dot{\tilde{x}}' = -J\tilde{x}' + \tilde{A}f(J\tilde{x}') + \tilde{B}\tilde{u} + \tilde{I} &\quad (7) \end{aligned}$$

$$\dot{\tilde{x}}' = -\tilde{x}' + J^{-1}\tilde{A}f(J\tilde{x}') + J^{-1}\tilde{B}\tilde{u} + J^{-1}\tilde{I} = F'(\tilde{x}') \quad (8)$$

The Jacobian matrix of  $F'$  is:

$$DF'(\tilde{x}') = J^{-1}\tilde{A}Df(J\tilde{x}')J - U \quad (9)$$

---

<sup>2</sup>we use the symbol  $\approx$  since in the following proofs, we will assume  $\hat{f}(x_i)$  to be a smooth, strictly increasing and odd approximation of the piecewise linear function.

where  $U$  denotes the identity matrix. Note that  $Df$  and  $J$  are both diagonal matrices, and thus they commute. Noting that  $J^{-1} = J$ , we have:

$$DF'(\tilde{x}') = J\tilde{A}JDf(J\tilde{x}') - U \quad (10)$$

So for  $i \neq j$ ,

$$\frac{\partial F'_i(\tilde{x}')}{\partial \tilde{x}'_j} = (J\tilde{A}J)_{ij} \left. \frac{df(v)}{dv} \right|_{[J\tilde{x}']_j} \quad (11)$$

So the system in (8) is cooperative and irreducible if and only if  $\tilde{A}' = J\tilde{A}J$  is nonnegative in the off-diagonal elements and is irreducible.

**Theorem 5.1** *The system (8) is stable almost everywhere if  $\tilde{A}'$  is nonnegative in the off-diagonal elements and irreducible.*

**Proof:** the proof is similar to that of lemma 1 in [3]. First we note that from any fixed  $\tilde{x}(0)$ , the state vector  $\tilde{x}$  in (5) has a bounded forward orbit by theorem 1 in [1], and therefore,  $\tilde{x}'$  has a bounded forward orbit.  $\tilde{x}'$  is an equilibrium point of (8) if and only if  $J\tilde{x}'$  is an equilibrium point of (5). Since the system (8) is cooperative and irreducible, theorem 5.1 follows from [4]. ■

If the transformed system is stable almost everywhere then the original system is also stable almost everywhere. It is clear that  $\tilde{A}$  is irreducible if and only if  $J\tilde{A}J$  is irreducible. So we need to find a  $J$  in the diagonal form described above such that  $J\tilde{A}J$  is an off-diagonal nonnegative matrix.

$$(J\tilde{A}J)_{ij} = (-1)^{n_i}(\tilde{A}J)_{ij} = (-1)^{n_i}\tilde{A}_{ij}(-1)^{n_j} = (-1)^{n_i+n_j}\tilde{A}_{ij} \quad (12)$$

The matrix  $\tilde{A}$  results from a space-invariant template. Assume that for all  $i \neq j$ ,  $\tilde{A}_{ij} \neq 0$ . Given this assumption, and the requirement that  $J\tilde{A}J$  has nonnegative off-diagonal elements, some properties of  $J$  can be obtained.  $\tilde{A}_{ij} \neq 0$  and  $(J\tilde{A}J)_{ij} \geq 0$  for all  $i \neq j$  implies that:

$$(-1)^{n_i+n_j}\tilde{A}_{ij} = |\tilde{A}_{ij}| \quad (13)$$

Let  $i = \sigma(a, b)$ ,  $j = \sigma(a+l, b)$ ,  $k = \sigma(a+2l, b)$  for some  $1 \leq a \leq M-2l$ ,  $1 \leq b \leq N$  and  $l = 1, \dots, \lfloor (M-1)/2 \rfloor$ . Because of spacial invariance,  $\tilde{A}_{ij} = \tilde{A}_{jk}$  and we have:

$$(-1)^{n_i+n_j}\tilde{A}_{ij} = |\tilde{A}_{ij}| = |\tilde{A}_{jk}| = (-1)^{n_j+n_k}\tilde{A}_{jk} = (-1)^{n_j+n_k}\tilde{A}_{ij} \quad (14)$$

Consequently, we have:

$$(-1)^{n_i} = (-1)^{n_k} \Rightarrow n_i = n_k \quad (15)$$

The same conclusion follows if we take  $i = \sigma(a, b)$ ,  $j = \sigma(a, b+l)$ ,  $k = \sigma(a, b+2l)$  for some  $1 \leq a \leq M$ ,  $1 \leq b \leq N-2l$  and  $l = 1, \dots, \lfloor (N-1)/2 \rfloor$ . Therefore we have the following sets of constraints on  $J$ :

$$n_{\sigma(a,b)} = n_{\sigma(a+2l,b)}, 1 \leq a \leq M-2l, 1 \leq b \leq N, l = 1, \dots, \lfloor (M-1)/2 \rfloor \quad (16)$$

$$n_{\sigma(a,b)} = n_{\sigma(a,b+2l)}, 1 \leq a \leq M, 1 \leq b \leq N-2l, l = 1, \dots, \lfloor (N-1)/2 \rfloor \quad (17)$$

This gives us 5 possible choices for  $J$ . From all the sign-changing transformations, only these 5 have any chance of generating a cooperative system. Two of them,  $J = \pm U$ , gives  $\tilde{A}' = \tilde{A}$ . The other three will be discussed in more details.

**Remark 1:** A transformation that changes all the states to their negatives amounts to  $J$  being equal to  $-U$ , and therefore  $\tilde{A}' = \tilde{A}$ , which does not help us in determining the stability of the system.

**Remark 2:** The 5 choices for  $J$  were found from the two sets of constraints (16) and (17) which in turn were derived from the space-invariance of the templates and the absence of zeros in the off diagonal elements of  $\tilde{A}$ . These  $J$ 's will also yield correct results if there are some zero-elements in the off-diagonal elements of  $\tilde{A}$ . If we are restricting ourselves to considering templates with zero-elements in certain locations, i.e.  $\tilde{A}$  has zeros in some off-diagonal entries, then some of the constraints might not be necessary and more choices for  $J$  can then be found. We will demonstrate that later in the paper.

**Remark 3:**  $\tilde{I}$  is assumed to be constant and  $\tilde{B}$  is assumed to be generated by a space-invariant B-template, since they correspond to a CNN with space-invariant templates. For  $J \neq U$ ,  $J^{-1}\tilde{B}$  need not correspond to a space-invariant B-template and  $J^{-1}\tilde{I}$  need not be a constant vector and (8) need not correspond to the repacked equation of a space-invariant CNN.

**Remark 4:** There are other constraints on  $J$  of the form

$$n_{\sigma(a,b)} = n_{\sigma(a \pm 2l, b \pm 2m)}, 1 \leq a \leq M-2l, 1 \leq b \leq N-2m \\ l = 1, \dots, \lfloor (M-1)/2 \rfloor, m = 1, \dots, \lfloor (N-1)/2 \rfloor \quad (18)$$

but they are equivalent to (16) and (17).

$\tilde{A}'$  generated by the 3 transformations is space-invariant in the sense that a space-invariant cloning template  $A'(i, j; k, l)$  generates  $\tilde{A}'$  through  $\sigma$ . To simplify notations, let us return to state equation (4). The transformation will now simply be:

$$v_{x'_{ij}} = v_{x_{ij}} \cdot (-1)^{n_{\sigma(i,j)}} \quad (19)$$

Let us denote the output variables after the transformation by  $v_{y'_{ij}} = \hat{f}(v_{x'_{ij}})$ . The state equation after the transformation is:

$$C \frac{dv_{x'_{ij}}(t)}{dt} = -\frac{1}{R'_x} v_{x'_{ij}}(t) + \sum_{k,l} A'(i, j; k, l) v_{y'_{kl}}(t)$$

$$+ \sum_{k,l} B'(i, j; k, l) v_{u_{kl}}(t) + I'_{ij} \quad (20)$$

For now, let us only consider  $3 \times 3$  templates.

(a) *transformation 1.*  $v_{x'_{ij}}(t) = v_{x_{ij}}(t) \cdot (-1)^j$ , i.e.  $v_{x'_{ij}}(t) = v_{x_{ij}}(t)$  if  $j$  is even,  $v_{x'_{ij}}(t) = -v_{x_{ij}}(t)$  if  $j$  is odd. It follows that the cells with their states changed to their negatives form alternating columns. The effect on the A-templates is depicted as follows:

$$\begin{array}{|c|c|c|} \hline +a & +b & +c \\ \hline +d & +e & +f \\ \hline +g & +h & +i \\ \hline \end{array} \quad A \quad \rightarrow \quad \begin{array}{|c|c|c|} \hline -a & +b & -c \\ \hline -d & +e & -f \\ \hline -g & +h & -i \\ \hline \end{array} \quad A'$$

Proof:  $v_{y'_{ij}}(t) = \hat{f}(v_{x_{ij}}(t))$ , and  $\hat{f}$  is odd. So if  $v_{x'_{ij}}(t) = -v_{x_{ij}}(t)$ , then  $v_{y'_{ij}}(t) = -v_{y_{ij}}(t)$ .

Suppose  $j$  is even; then  $v_{x'_{ij}}(t) = v_{x_{ij}}(t)$ .

$$\begin{aligned} \frac{dv_{x'_{ij}}(t)}{dt} &= \frac{dv_{x_{ij}}(t)}{dt} = A(i, j; i+1, j+1) v_{y_{(i+1)(j+1)}}(t) + \dots \\ &= A(i, j; i+1, j+1) (-v_{y'_{(i+1)(j+1)}}(t)) + \dots \\ &= A'(i, j; i+1, j+1) v_{y'_{(i+1)(j+1)}}(t) + \dots \end{aligned} \quad (21)$$

where the symbol  $+\dots$  indicates the *remaining terms* which are not relevant to our proof here.

Therefore  $A'(i, j; i+1, j+1) = -A(i, j; i+1, j+1)$ . The same argument is valid when  $i+1$  is replaced by  $i$ , or  $i-1$ , and when  $j+1$  is replaced by  $j-1$  ( $j+1$  and  $j-1$  are both odd).

$$\begin{aligned} \frac{dv_{x'_{ij}}(t)}{dt} &= \frac{dv_{x_{ij}}(t)}{dt} = A(i, j; i+1, j) v_{y_{(i+1)j}}(t) + \dots \\ &= A(i, j; i+1, j) v_{y'_{(i+1)j}}(t) + \dots \\ &= A'(i, j; i+1, j) v_{y'_{(i+1)j}}(t) + \dots \end{aligned} \quad (22)$$

Therefore  $A'(i, j; i+1, j) = A(i, j; i+1, j)$ . The same argument is valid when  $i+1$  is replaced by  $i-1$  or  $i$ .

Suppose  $j$  is odd; then  $v_{x'_{ij}}(t) = -v_{x_{ij}}(t)$ .

$$\begin{aligned} \frac{dv_{x'_{ij}}(t)}{dt} &= -\frac{dv_{x_{ij}}(t)}{dt} = -A(i, j; i+1, j+1) v_{y_{(i+1)(j+1)}}(t) + \dots \\ &= -A(i, j; i+1, j+1) v_{y'_{(i+1)(j+1)}}(t) + \dots \\ &= A'(i, j; i+1, j+1) v_{y'_{(i+1)(j+1)}}(t) + \dots \end{aligned} \quad (23)$$

Therefore  $A'(i, j; i+1, j+1) = -A(i, j; i+1, j+1)$ . The same argument is valid when  $i+1$  is replaced by  $i$ , or  $i-1$ , and when  $j+1$  is replaced by  $j-1$  ( $j+1$  and  $j-1$  are both even).

$$\begin{aligned}
\frac{dv_{x'_{ij}}(t)}{dt} &= -\frac{dv_{x_{ij}}(t)}{dt} = -A(i, j; i+1, j)v_{y_{(i+1),j}}(t) + \dots \\
&= -A(i, j; i+1, j)(-v_{y'_{(i+1),j}}(t)) + \dots \\
&= A'(i, j; i+1, j)v_{y'_{(i+1),j}}(t) + \dots
\end{aligned} \tag{24}$$

Therefore  $A'(i, j; i+1, j) = A(i, j; i+1, j)$ . The same argument is valid when  $i+1$  is replaced by  $i-1$  or  $i$ . ■

(b) *transformation 2.*  $v_{x'_{ij}}(t) = v_{x_{ij}}(t) \cdot (-1)^i$ , i.e.  $v_{x'_{ij}}(t) = v_{x_{ij}}(t)$  if  $i$  is even,  $v_{x'_{ij}}(t) = -v_{x_{ij}}(t)$  if  $i$  is odd. It follows that the cells with their states changed to their negatives form alternating rows. The effect on the A-templates is depicted below:

$$\begin{array}{|c|c|c|} \hline +a & +b & +c \\ \hline +d & +e & +f \\ \hline +g & +h & +i \\ \hline \end{array} \rightarrow \begin{array}{|c|c|c|} \hline -a & -b & -c \\ \hline +d & +e & +f \\ \hline -g & -h & -i \\ \hline \end{array}$$

$A \qquad A'$

The proof is similar to that of the previous transformation. In essence, this is transformation 1 rotated 90 degrees.

(c) *transformation 3.*  $v_{x'_{ij}}(t) = v_{x_{ij}}(t) \cdot (-1)^{(i+j)}$ , i.e.  $v_{x'_{ij}}(t) = v_{x_{ij}}(t)$  if  $i+j$  is even,  $v_{x'_{ij}}(t) = -v_{x_{ij}}(t)$  if  $i+j$  is odd. It follows that the cells with their states changed to their negatives form a checkerboard pattern.

The effect on the A-templates is depicted as follows:

$$\begin{array}{|c|c|c|} \hline +a & +b & +c \\ \hline +d & +e & +f \\ \hline +g & +h & +i \\ \hline \end{array} \rightarrow \begin{array}{|c|c|c|} \hline +a & -b & +c \\ \hline -d & +e & -f \\ \hline +g & -h & +i \\ \hline \end{array}$$

$A \qquad A'$

Proof: suppose  $i+j$  is even; then  $v_{x'_{ij}}(t) = v_{x_{ij}}(t)$ .

$$\begin{aligned}
\frac{dv_{x'_{ij}}(t)}{dt} &= \frac{dv_{x_{ij}}(t)}{dt} = A(i, j; i+1, j+1)v_{y_{(i+1)(j+1)}}(t) + \dots \\
&= A(i, j; i+1, j+1)v_{y'_{(i+1)(j+1)}}(t) + \dots \\
&= A'(i, j; i+1, j+1)v_{y'_{(i+1)(j+1)}}(t) + \dots
\end{aligned} \tag{25}$$

Therefore  $A'(i, j; i+1, j+1) = A(i, j; i+1, j+1)$ . The same argument is valid when  $i+1$  is replaced by  $i-1$ , or when  $j+1$  is replaced by  $j-1$  or when considering  $A'(i, j; i, j)$  (the sum of the second pair of indices stays even)

$$\begin{aligned}\frac{dv_{x'_{ij}}(t)}{dt} &= \frac{dv_{x_{ij}}(t)}{dt} = A(i, j; i+1, j)v_{y_{(i+1)j}}(t) + \dots \\ &= A(i, j; i+1, j)(-v_{y'_{(i+1)j}}(t)) + \dots \\ &= A'(i, j; i+1, j)v_{y'_{(i+1)j}}(t) + \dots\end{aligned}\quad (26)$$

Therefore  $A'(i, j; i+1, j) = -A(i, j; i+1, j)$ . The same argument is valid when  $i+1$  is replaced by  $i-1$ . It is valid also when  $i+1$  is replaced by  $i$ , and  $j$  in the second set of coordinates is replaced by  $j+1$  or  $j-1$ . (the sum of the second set of indices stays even)

Suppose  $i+j$  is odd; then  $v_{x'_{ij}}(t) = -v_{x_{ij}}(t)$ .

$$\begin{aligned}\frac{dv_{x'_{ij}}(t)}{dt} &= -\frac{dv_{x_{ij}}(t)}{dt} = -A(i, j; i+1, j+1)v_{y_{(i+1)(j+1)}}(t) + \dots \\ &= -A(i, j; i+1, j+1)(-v_{y'_{(i+1)(j+1)}}(t)) + \dots \\ &= A'(i, j; i+1, j+1)v_{y'_{(i+1)(j+1)}}(t) + \dots\end{aligned}\quad (27)$$

Therefore  $A'(i, j; i+1, j+1) = A(i, j; i+1, j+1)$ . The same argument is valid when  $i+1$  is replaced by  $i-1$  or when  $j+1$  is replaced by  $j-1$  or when considering  $A'(i, j; i, j)$  (the sum of the second pair of indices remains odd)

$$\begin{aligned}\frac{dv_{x'_{ij}}(t)}{dt} &= -\frac{dv_{x_{ij}}(t)}{dt} = -A(i, j; i+1, j)v_{y_{(i+1)j}}(t) + \dots \\ &= -A(i, j; i+1, j)v_{y'_{(i+1)j}}(t) + \dots \\ &= A'(i, j; i+1, j)v_{y'_{(i+1)j}}(t) + \dots\end{aligned}\quad (28)$$

Therefore  $A'(i, j; i+1, j) = -A(i, j; i+1, j)$ . The same argument is valid when  $i+1$  is replaced by  $i-1$ . It is also valid when  $i+1$  is replaced by  $i$  and  $j$  in the second set of coordinates is replaced by  $j-1$  or  $j+1$ . (the sum of the second pair of indices stays even) ■

We can now summarize the above results into the form of a theorem. Note that  $A'(i, j; k, l)$  is positive cell-linking if and only if  $\tilde{A}'$  is off-diagonal nonnegative and irreducible:

**Theorem 5.2** *If through one of the above 3 transformations on  $A(i, j; k, l)$  the resulting  $A'(i, j; k, l)$  is positive cell-linking, then the CNN with the template  $A(i, j; k, l)$  is stable almost everywhere.*

The main idea is that the transformation either changes the state of a cell to its negative or it does not change the state of a cell. Consider two cells  $(i, j)$

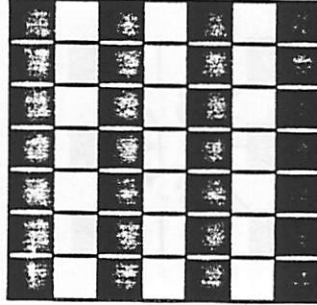


Figure 5: Under transformation 1, black cells have their states reversed, while white cells remain unchanged.

and  $(j,k)$  connected by a template element  $A(i,j;k,l)$ . The cells are connected by an edge in  $\Gamma$ . If both cells' states are changed to their negatives by the transformation, then the connection between these two cells remain the same after the transformation. ( $A'(i,j;k,l) = A(i,j;k,l)$ ) The same result occurs if both cells' state remain unchanged. If one cell's state is changed to its negative, while the other cell's state remain unchanged, then the connection between these two cells is changed to its negative. ( $A'(i,j;k,l) = -A(i,j;k,l)$ ) So by looking at how a cell is changed by the transformation relative to the surrounding cells, we can determine the transformation's effect on the connections  $A(i,j;k,l)$  and  $\Gamma$ .

For example, let us consider transformation 1. In Fig. 5, the dark cells correspond to cells that have their state variables changed to their negatives, while the white cells correspond to cells that have their state variables left alone. Consider first an arbitrary white cell, which we shall call the center cell, and it's neighbors as it would appear in  $\Gamma$ . (In Fig. 6, the labels have been omitted and only the edges pointing towards the center cell is shown.) The transformation does not change the state of the center cell. The cells immediately to the left and to the right of the center cell have their states changed, so all the edges pointing towards the white cell from its immediate right and left neighbors have changed sign. The right and left (with respect to the center) elements on the A-template of the center cell corresponds to these edges, and are also changed to their negatives. The cells above and below the center cell remain the same, and thus the elements above and below the center on the A-template of the center cell does not change. Similarly, the diagonal elements of the A-template is changed to their negatives. So the effect of this transformation on the A-template can be read off directly by looking at the difference in color between

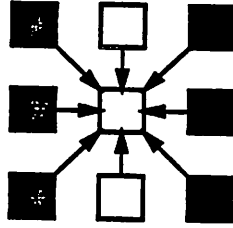


Figure 6: Cells on the left and right of the center cell have their state changed to their negatives.

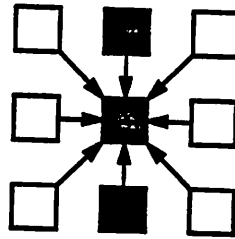


Figure 7: Cells in the center columns has its states changed, while the cells on the left and right are not.

the center cell and its neighbors in Fig. 6.

Consider next an arbitrary dark cell (which we call the center cell now) and it's neighbors as it would appear in  $\Gamma$ (Fig. 7) The center cell itself has its state changed to its negative, while the cells to the left and to the right of the center cell are left alone. So the left elements and the right elements (with respect to the center) of the A-template of the center cell is changed to its negative. The cells immediately above and below the center cell also change to their negatives along with the center cell, so the element above and below the center on the A-template of the center cell does not change. Again, the effect on the A-template is apparent from the color pattern of Fig. 7.

The effect of the transformation on the A-template is the same in both cases. This is due to the fact that these transformations preserve space-invariance of



the A-templates. We will illustrate this using a concrete numerical example, where the template  $A$  is changed to  $A'$  by transformation 1:

$$\begin{array}{|c|c|c|} \hline -1 & +1 & -1 \\ \hline -1 & +2 & -1 \\ \hline -1 & +1 & -1 \\ \hline \end{array} \quad \rightarrow \quad \begin{array}{|c|c|c|} \hline +1 & +1 & +1 \\ \hline +1 & +2 & +1 \\ \hline +1 & +1 & +1 \\ \hline \end{array}$$

$A \qquad \qquad \qquad A'$

Consider first an arbitrary cell  $(5,6)$ ;  $v_{x'_{56}}(t) = v_{x_{56}}(t)$ . The neighbors' coordinates are:

$(\bar{4}, 5)$	$(4, 6)$	$(\bar{4}, 7)$
$(\bar{5}, 5)$	$(5, 6)$	$(\bar{5}, 7)$
$(\bar{6}, 5)$	$(6, 6)$	$(\bar{6}, 7)$

A bar above the coordinates indicates that that cell will be changed to it's negative by the transformation.

$$\begin{aligned} \frac{dv_{x'_{56}}(t)}{dt} &= \frac{dv_{x_{56}}(t)}{dt} = A(5, 6; 6, 7)v_{y_{67}}(t) + \dots \\ &= v_{y'_{67}}(t) + \dots \\ &= A'(5, 6; 6, 7)v_{y'_{67}}(t) + \dots \end{aligned} \tag{29}$$

Therefore  $A'(5, 6; 6, 7) = 1$ . Same argument is valid for  $A'(5, 6; 5, 7)$ ,  $A'(5, 6; 4, 7)$ ,  $A'(5, 6; 4, 5)$ ,  $A'(5, 6; 5, 5)$ ,  $A'(5, 6; 6, 5)$ .

$$\begin{aligned} \frac{dv_{x'_{56}}(t)}{dt} &= \frac{dv_{x_{56}}(t)}{dt} = A(5, 6; 6, 6)v_{y_{66}}(t) + \dots \\ &= 1 \cdot v_{y'_{66}}(t) + \dots \\ &= A'(5, 6; 6, 6)v_{y'_{66}}(t) + \dots \end{aligned} \tag{30}$$

Therefore  $A'(5, 6; 6, 6) = 1$ . Same argument is valid for  $A'(5, 6; 4, 6)$ ,  $A'(5, 6; 5, 6)$ ,  $A'(5, 6; 6, 6)$ .

Consider next cell  $(5,7)$ , the cell to the right of cell  $(5,6)$ ;  $v_{x'_{57}}(t) = -v_{x_{57}}(t)$ . The neighbors' coordinates are:

$(4, 6)$	$(\bar{4}, 7)$	$(4, 8)$
$(5, 6)$	$(\bar{5}, 7)$	$(5, 8)$
$(6, 6)$	$(\bar{6}, 7)$	$(6, 8)$

Again, a bar above the coordinates indicates that the cell will be changed to its negatives by the transformation.

$$\begin{aligned}
\frac{dv_{x'_{57}}(t)}{dt} &= -\frac{dv_{x_{57}}(t)}{dt} = -A(5, 7; 6, 8)v_{y_{68}}(t) + \dots \\
&= 1 \cdot v_{y'_{68}}(t) + \dots \\
&= A'(5, 7; 6, 8)v_{y'_{68}}(t) + \dots
\end{aligned} \tag{31}$$

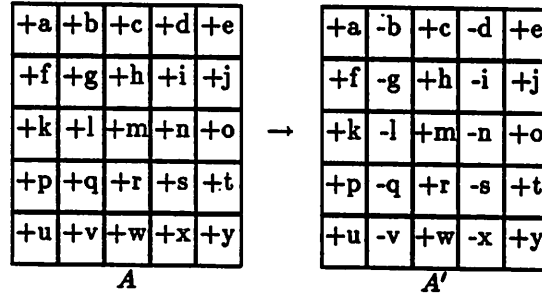
Therefore  $A'(5, 7; 6, 8) = 1$ . Same argument is valid for  $A'(5, 7; 5, 8)$ ,  $A'(5, 7; 4, 8)$ ,  $A'(5, 7; 4, 6)$ ,  $A'(5, 7; 5, 6)$ ,  $A'(5, 7; 6, 6)$ .

$$\begin{aligned}
\frac{dv_{x'_{57}}(t)}{dt} &= -\frac{dv_{x_{57}}(t)}{dt} = -A(5, 7; 6, 7)v_{y_{67}}(t) + \dots \\
&= -1 \cdot (-v_{y'_{67}}(t)) + \dots \\
&= A'(5, 7; 6, 7)v_{y'_{67}}(t) + \dots
\end{aligned} \tag{32}$$

Therefore  $A'(5, 7; 6, 7) = 1$ . Same argument is valid for  $A'(5, 7; 4, 7)$ ,  $A'(5, 7; 5, 7)$ .

## 6 Bigger templates and hexagonal templates

The above three transformations of templates are similar when extended to larger size templates. For example, transformation 1 has the following effect on a  $5 \times 5$  template:



The same technique can be applied to other network topologies as well. For example, in a hexagonal network, we would have a transformation that change a template as in Fig. 8. There are also two other transformations that are just the transformation in Fig. 8 rotated 60 and 120 degrees.

## 7 Strictly sign-symmetric templates

All the stability results we obtain so far are for cell-linking templates. We will now introduce a class of templates that is not necessarily cell-linking.

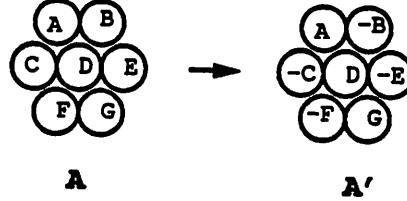


Figure 8: Effect of a transformation on a hexagonal template.

**Definition 7.1** A CNN is called *strictly sign-symmetric* if whenever  $A(i, j; k, l) \neq 0$ ,  $A(i, j; k, l)A(k, l; i, j) > 0$ .<sup>3</sup>

In view of the repacked equation (5), this is equivalent to saying that  $\tilde{A}_{ij}\tilde{A}_{ji} > 0$  if  $\tilde{A}_{ij} \neq 0$ . Because of space-invariance, this means that the templates are sign-symmetric with respect to the center element, i.e.  $A(i, j; i+m, j+n)A(i, j; i-m, j-n) > 0$  if  $A(i, j; i+m, j+n) \neq 0$ . For such a template, the sign of each *non-zero* element is identical to the sign of its corresponding symmetric (with respect to the center element) element. We will also call the associated templates strictly sign-symmetric. For example, in table 1, only template (a),(b),(c) and (f) are strictly sign-symmetric. A strictly sign-symmetric template generates a symmetric signed interaction graph.

In our next lemma, we say a CNN is composed of *independent* subsystems if the state variables can be partitioned into  $n$  subsets of state variables  $S_1, \dots, S_n$ , such that  $A(i, j; k, l) = 0$  for  $\text{cell}(i, j) \in S_a$ ,  $\text{cell}(k, l) \in S_b$  and  $S_a \neq S_b$ . In other words, the state of cells in one subset in the partition is independent of the state of cells in other subsets in the partition.

**Lemma 7.1** A CNN composed of independent subsystems is stable almost everywhere if each subsystem is stable almost everywhere.

**Proof:** Consider first a system composed of two independent subsystems. Since the states are bounded, given that the initial conditions are taken from a bounded set[1], we denote the state space of the system to be the cartesian product of closed interval  $[a, a+b]$ ,  $b > 0$ ; namely  $[a, a+b]^n$ . Similarly, let the state space of subsystem 1 be  $[a, a+b]^k$ , and that of subsystem 2 be  $[a, a+b]^{n-k}$ ,  $b > 0$ . Assume that the state variables of the whole system is composed of first

<sup>3</sup>This definition of "strict sign-symmetry" is more restrictive than that of "sign-symmetry" defined in [5]

the state variables of subsystem 1, and then followed by the state variables of subsystem 2. Let  $E_i$  be the set of initial values in which subsystem  $i$  is not stable, where  $i \in \{1, 2\}$ . Let  $E$  be the set of initial values in which the entire system is not stable. An initial state  $x$  is not stable for the system if the subvector of the first  $k$  coordinates belongs to  $E_1$  or the subvector of the last  $n - k$  coordinates belongs to  $E_2$ . Let  $\alpha \subseteq [a, a + b]^k$  be a covering of  $E_1$  with measure  $\epsilon$  then  $\alpha' = \{(x_1, \dots, x_n) : (x_1, \dots, x_k) \in \alpha\}$  has measure  $b^{n-k}\epsilon$ . Similarly, let  $\beta \subseteq [a, a + b]^{n-k}$  be a covering of  $E_2$  with measure  $\epsilon$  then  $\beta' = \{(x_1, \dots, x_n) : (x_{k+1}, \dots, x_n) \in \beta\}$  has measure  $b^k\epsilon$ . Now  $\alpha' \cup \beta'$  is a covering of  $E$  with measure  $\leq (b^{n-k} + b^k)\epsilon$ . Since  $\epsilon$  can be made as small as possible,  $E$  has measure zero. So the whole system is stable almost everywhere. The proof for a finite number of subsystems is similar. ■

**Theorem 7.1** *A positive strictly sign-symmetric CNN is stable almost everywhere*

**Proof:** As shown earlier a symmetric graph can be decomposed into maximally irreducible subgraphs that are disconnected from each other. Because all the edges have positive labels, the CNN can be decomposed into independent positive irreducible subnetworks and each subnetwork has been shown to be stable almost everywhere [3], [4]. By lemma 7.1, the whole CNN is completely stable almost everywhere. ■

For example, template (f) in table 1 corresponds to a  $\Gamma$  with two positive maximally irreducible subgraphs. So the CNN corresponding to that template is stable almost everywhere.

Theorem 5.1 and theorem 5.2 are still true when the words “irreducible” and “cell-linking” are replaced by “strictly sign-symmetric”. Note that the property of “cell-linking” and “strictly sign-symmetric” is preserved under the three sign-changing transformations presented earlier. So using these transformations, only cell-linking templates can be transformed into a positive cell-linking template, and only strictly sign-symmetric templates can be transformed into a positive strictly sign-symmetric template.

Using the three sign-changing transformations, and theorem 7.1, we can deduce that the following classes of  $3 \times 3$  strictly sign-symmetric templates are stable almost everywhere.<sup>4</sup>

In the following descriptions, the elements refer to the elements of the templates, not including the center. In the figures, the number above the arrow indicates the type of transformation (1, 2, or 3) used. N indicates the corresponding weight is non-positive, and P indicates that the corresponding weight is non-negative. A + and – indicates positive and negative weights respectively. The choice of the weights must be kept consistent with the definition of strict sign-symmetry.

---

<sup>4</sup>Most of these  $3 \times 3$  strictly sign-symmetric templates are cell-linking, and the stability can be deduced without using theorem 7.1, but we would like to illustrate the technique used. For bigger templates, strictly sign-symmetric templates are not necessarily cell-linking.

1. corner elements are zero

0	P	0
N	A	N
0	P	0

 $\xrightarrow{1}$ 

0	P	0
P	A	P
0	P	0

The four possible combinations are:

0	+	0
-	A	-
0	+	0

0	0	0
-	A	-
0	0	0

0	+	0
0	A	0
0	+	0

0	0	0
0	A	0
0	0	0

0	N	0
P	A	P
0	N	0

 $\xrightarrow{2}$ 

0	P	0
P	A	P
0	P	0

Some examples are:

0	-	0
+	A	+
0	-	0

0	0	0
+	A	+
0	0	0

0	-	0
0	A	0
0	-	0

0	N	0
N	A	N
0	N	0

 $\xrightarrow{3}$ 

0	P	0
P	A	P
0	P	0

An example:

0	-	0
-	A	-
0	-	0

2. corner elements are nonnegative, while the rest is nonpositive

P	N	P
N	A	N
P	N	P

 $\xrightarrow{3}$ 

P	P	P
P	A	P
P	P	P

Some examples are:

0	-	+
-	A	-
+	-	0

+	-	+
-	A	-
+	-	+

0	0	+
-	A	-
+	0	0

+	-	+
0	A	0
+	-	+

3. every element is nonpositive, except two nonnegative elements aligned in a row or a column.

N	P	N
N	A	N
N	P	N

 $\xrightarrow{1}$ 

P	P	P
P	A	P
P	P	P

Some examples are:

0	+	-
-	A	-
-	+	0

-	0	-
-	A	-
-	0	-

-	+	-
0	A	0
-	+	-

-	+	0
0	A	0
0	+	-

N	N	N
P	A	P
N	N	N

 $\xrightarrow{2}$ 

P	P	P
P	A	P
P	P	P

Some examples are:

-	0	-
0	A	0
-	0	-

-	-	0
0	A	0
0	-	-

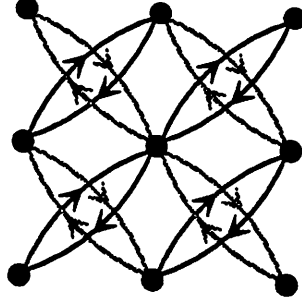


Figure 9: Signed interaction graph.

The following templates are also stable almost everywhere:

-	0	+
0	A	0
+	0	-

+	0	-
0	A	0
-	0	+

One way to show that they are stable almost everywhere is by constructing  $\Gamma$  of the first template (Fig. 9). By separating the two maximally irreducible subgraphs, we see that each component is topologically equivalent to the signed interaction graph of a strictly sign-symmetric template with the corner elements equal to zero, which we know is stable almost everywhere (Fig. 10). Since the stability results we obtained are solely dependent on the template  $A(i, j; k, l)$  or equivalent on  $\Gamma$ , the system corresponding to each component is stable almost everywhere and so is the whole system by lemma 7.1. By way of one of the three transformations, the second template can also be shown to be stable almost everywhere.

There are only 5 state transformations (2 of them trivial) of the type discussed in section 5 such that theorem 5.2 can be used on all types of templates. Other transformations can exist if we restrict ourselves to templates with zero elements in certain locations. To illustrate this, we will give an alternate proof of the stability of the first template in the pair shown above.

Because the template has some zero elements, the following state transformation will work in theorem 5.2.

*Transformation 4:*  $v_{x'_{ij}}(t) = -v_{x_{ij}}(t)$  if  $i + j \equiv 0 \pmod{4}$ , or  $i + j \equiv 1 \pmod{4}$ , and  $v_{x'_{ij}}(t) = v_{x_{ij}}(t)$  otherwise. The cells that have their states changed to their negatives are shown in black in Fig. 11. The effect on the A-template is:

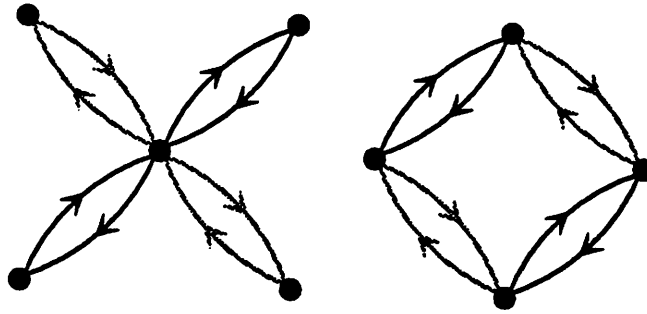


Figure 10: The signed interaction graph in Fig. 11 can be separated into two maximally irreducible subgraphs.

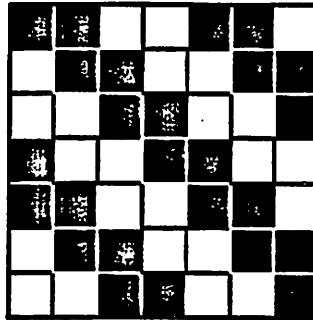
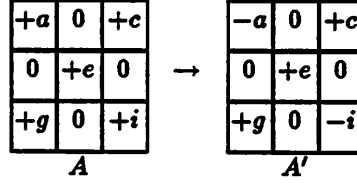


Figure 11: Pattern of how the cells is transformed using transformation 4. Black cells have their states changed to their negatives. While cells are left unchanged.





This transformation changes the A-template (with  $a < 0$  and  $i < 0$ ) into a positive strictly sign-symmetric template which we know is stable almost everywhere.

## 8 Acyclic $\Gamma$

**Theorem 8.1** *A CNN with an acyclic  $\Gamma$  and  $A(i, j; i, j) > R_x^{-1}$  is completely stable.*

**Proof:** because  $\Gamma$  is acyclic, there exists a set of cells such that there are no edges going towards it. Since they receive no input from other cells and the external input is constant these cells converge to an equilibrium. As shown in [1],  $A(i, j; i, j) > R_x^{-1}$  implies that stable equilibria have magnitude greater than 1. The states are bounded and the output of these cells will not change after a finite time. Delete those cells and the edges coming out of them, and the resulting graph will have another set of cells such that there are no edges going towards it. The only varying influence or input acting on these cells are from cells whose output will not change after a finite time. So these cells also converge with an unchanging output after a finite time. This argument can be repeated until all the cells have been shown to converge. ■

A sufficient condition for a template to generate an acyclic  $\Gamma$  is the following:

**Theorem 8.2** *A template such that the white portion in Fig. 12(excluding the center) has only zero elements generates a CNN with an acyclic  $\Gamma$ .*

**Proof:** We need to show that there are no cycles in  $\Gamma$ . Imagine the cells are arranged on a regular rectangular lattice in cartesian space with the edges of  $\Gamma$  being straight vectors connecting the nodes. Then the edges have a certain direction that we can decompose into a horizontal and vertical component. The hypothesis in theorem 8.2 corresponds to the edges in  $\Gamma$  having a horizontal direction  $\geq 0$ . Now we show that a cycle must include a edge with horizontal direction  $> 0$ . Suppose not, then a cycle must consists solely of edges with horizontal direction  $= 0$ . The only edge that has no horizontal direction is an edge pointing straight up. Such a path can never be a cycle. So a cycle must include edges with horizontal direction  $> 0$ . But there are no edges with horizontal direction  $< 0$ . So you move farther and farther away horizontally in such a path. Therefore there are no cycles in the graph. ■

In this paper we have extended the stability results in [3] to a class of CNN templates that are not necessarily positive cell-linking. Among them is a subclass of strictly sign-symmetric templates. Other strictly sign-symmetric templates that has not yet been shown to be stable are the following:

## 9 Concluding remarks

Acyclic templates can neither be cell-linking nor strictly sign-symmetric. By considering an  $L$ -layer  $M \times N$  CNN as an  $L$  by  $M$  by  $N$  array of cells, the definition of a signed interaction graph can be applied to a multiple layer CNN. It is easy to show that the graph of a feedforward multiple layer CNN consisting of linear threshold layers [7] is acyclic.

+	+	-	+	+
+	-	+	+	+
+	+	+	+	+
+	+	+	+	+
+	+	+	+	+

For simplicity, we will call such a template acyclic. Of course, an acyclic template is still acyclic after rotation or reflection. An example of an acyclic template that satisfy the hypothesis of theorem 8.2 (after reflection) is the horizontal shadow detector (table 1(d)). Another example is the following template:

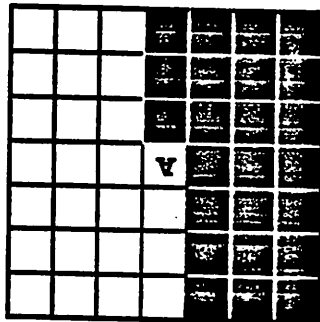


Figure 12: The white portion of the template(excluding the center) having only zero elements is a sufficient condition for a template to generate an acyclic  $L$ .

-	-	-	+	+	+	+	-	+	-	-	+	+	+	-	+	-
-	A	-	-	A	-	+	A	+	+	A	+	-	A	-	+	+
-	-	-	+	+	+	+	-	+	-	+	-	-	+	-	-	-

These four templates are equivalent and belong to the same equivalence class in the sense that they can be transformed into each other through rotations, reflections or the three transformations defined in section 5. If one of them can be shown to be stable almost everywhere (or unstable everywhere) then so are the other three.

Similarly, the following templates and its equivalent templates form another class of strictly sign-symmetric templates that have not been shown to be stable:

-	-	P
-	A	-
P	-	-

A third class consists of the following template and its equivalent templates:

+	0	-
+	A	+
-	0	+

These three classes, together with the templates in section 7, form all of the  $3 \times 3$  strictly sign-symmetric templates. Out of the 81 possible types of strictly sign-symmetric  $3 \times 3$  templates, 53 have been proved to be stable almost everywhere. The rest form the three classes above.

Combining the results in this paper and [3], we find that out of the 6561 possible types of  $3 \times 3$  templates with  $A(i, j; i, j) > R_{\varepsilon}^{-1}$ , 965 have been proved to be stable almost everywhere. This forms a relatively large but yet *incomplete* subset of the universe of *all* stable  $3 \times 3$  templates. Figure 13 illustrates the relationship between the various types of templates that are presently known to be stable almost everywhere. For the definitions of the different classes, see definition 2.4, 2.5, 7.1, and section 8. The yet unsolved problem is to identify the *complete* universe of *all* stable templates.

## 10 Acknowledgements

The authors would like to thank Mr. Bert Shi and Prof. Morris Hirsh for helpful discussions.

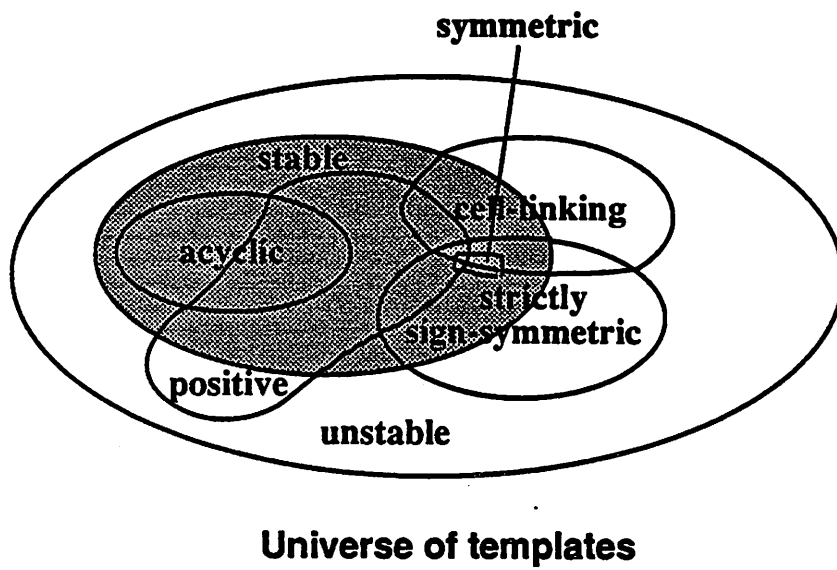


Figure 13: Venn diagram illustrating the relationship between the different classes of templates. The universe of templates stable almost everywhere is shown shaded.

## References

- [1] L. O. Chua and L. Yang, *Cellular neural networks: Theory*, IEEE Transactions on Circuits and Systems, Vol.35, pp. 1257-1272, 1988.
- [2] L. O. Chua and L. Yang, *Cellular neural networks: Applications*, IEEE Transactions on Circuits and Systems, Vol.35, pp. 1273-1290, 1988.
- [3] L. O. Chua and Tamás Roska, *Stability of a class of nonreciprocal cellular neural networks*, IEEE Transactions on Circuit and Systems, Vol. 37, pp. 1520-1527, 1990.
- [4] M. W. Hirsch, *Systems of differential equations that are competitive or cooperative II.: Convergence almost everywhere*, SIAM J. Math. Anal., Vol.16, pp. 423-439, 1985.
- [5] M. W. Hirsch, *Convergent activation dynamics in continuous time networks*, Neural Networks, Vol. 2, pp. 331-349, 1989.
- [6] M. W. Hirsh, *Convergence in Neural Nets*, IEEE First International Conference on Neural Networks, Vol. 2, ed. by M. Caudill and C. Butler, pp. 115-125, 1987.
- [7] L. O. Chua and B. E. Shi, *Multiple layer cellular neural networks: a tutorial*, to appear in Algorithms and Parallel VLSI Architectures, ed. by E.F. Deprettiere, Elsevier Science Publishers B. V., Amsterdam, 1991.
- [8] T. Matsumoto, L. O. Chua, H. Suzuki, *CNN cloning template: Connected component detector*, IEEE Transactions on Circuits and Systems, Vol. 37, pp. 633-635, 1990.
- [9] T. Matsumoto, L. O. Chua, R. Furukawa, *CNN cloning template: Hole-Filler*, IEEE Transactions on Circuits and Systems, Vol. 37, pp. 635-638, 1990.
- [10] T. Matsumoto, L. O. Chua, T. Yokohama, *Image Thinning with a Cellular Neural Network*, IEEE Transactions on Circuits and Systems, Vol. 37, pp. 638-640, 1990.
- [11] T. Matsumoto, L. O. Chua, H. Suzuki, *CNN cloning template: Shadow detector*, IEEE Transactions on Circuits and Systems, Vol. 37, pp. 1070-1073, 1990.
- [12] T. Roska, T. Boros, P. Thiran, L. O. Chua, *Detecting Simple Motion Using Cellular Neural Networks*, IEEE International Workshop on Cellular Neural Networks and Their Applications, pp. 127-138, 1990.